CdS Nanobelts on Si Substrate

Weifeng Liu, Chuangui Jin, Chong Jia, Lianzeng Yao, Weili Cai,* and Xiaoguang Li
Department of Materials Science and Engineering, University of Science and Technology of China, Hefei, Anhui 230026, P. R. China

(Received September 8, 2003; CL-030822)

CdS nanobelts were successfully synthesized by rapidly evaporating CdS nanoparticles. The nanobelts are single crystals with a hexagonal structure growing along the [001] direction. Photoluminescence measurement shows that the nanobelts have two emission bands around 517 and 735 nm, which should come from the intrinsic transition and the V_s^+ vacancies, respectively.

Cadmium sulfide, an important II–VI semiconductor, has a typical wide band gap of 2.42 eV at room temperature, and displays excellent optical properties. It has been studied extensively because of its wide applications in laser light-emitting diodes, solar cells and other optical devices based on its nonlinear properties.[1–4] CdS, as a famous luminescence material, shows various luminescence properties, such as photoluminescence (PL) and electroluminescence. It is well known that nanoscaled semiconductor materials show fantastic properties, and great efforts have been made to control their size, morphology, and crystallinity in order to obtain desired properties. Thus, a variety of CdS nanomaterials, such as nanorods, nanowires and nanotubes, have been fabricated[5–11] and investigated.

Nanobelts, a new family in the realm of 1-D nanomaterials, are regarded as an ideal system to fully understand dimensionally confined transport properties and may act as valuable units to construct nanodevices owing to their well-defined geometry. Many kinds of oxide nanobelts,[12,13] e.g., ZnO and CdO, and a few sulfide nanobelts[14] (such as ZnS) have been prepared so far. Recently, Liu et al. have synthesized belt-like nanostructured CdS via a low-temperature solvothermal route.[15] In this letter, we report the preparation of cadmium sulfide nanobelts using a simple thermal evaporation process. Their structural characterization and the PL property are also studied.

A silicon wafer (1×1 cm) was used as a substrate for the growth of CdS nanobelts. Before evaporation, the Si substrate was cleaned using a conventional treatment with HF, HCl/H_2O_2 and NH_4OH/H_2O_2 solution, respectively, and kept in ethanol for use. CdS nanopowder, as a precursor, was synthesized by mixing the saturated Na_2S and the $CdSO_4$ solutions together with magnetic stirring. The deposit was rinsed with deionized water, and then dried at 60 °C in air. The TEM images show the diameter of the nanoparticles is about 5 nm (not shown here). The CdS nanopowder put in a quartz vessel was placed into a quartz tube, and a cleaned Si substrate was placed next to the powder along to the downstream side of flowing argon. Prior to heating, the air in the quartz tube was pumped out, and then high-purity Ar was introduced. Repeating this process for three times to make sure the O_2 was eliminated. At last, the pressure was kept at about 1.6×10^4 Pa, and the quartz tube was rapidly heated to 900 °C (within about 5 min) with a constant Ar flowing rate (0.3 sccm). Held for 30 min, the power was then switched off and the quartz tube was cooled down to room temperature in the furnace. Yellow sponge-like products appeared on the surface of the Si substrate.

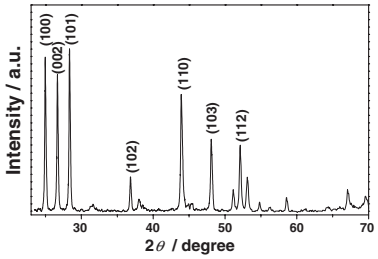

Figure 1. XRD pattern of CdS nanobelts.

Figure 1 shows the XRD pattern of the as-prepared CdS sample. It reveals that the products are pure hexagonal wurtzite CdS with lattice constants of $a = 4.123$ Å and $c = 6.674$ Å, which are very close to the data in the literature (JCPDS, No.77-2306). And, no byproducts are found.

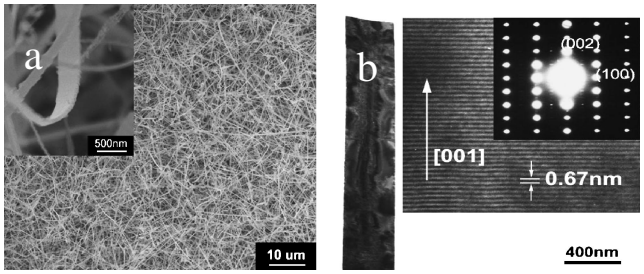

Figure 2. SEM and TEM images of CdS nanobelts. a) The top view of CdS nanobelts, the inset is a single nanobelt. b) The TEM image of a CdS nanobelt and its magnification, the inset is the corresponding ED pattern.

Figure 2 presents typical SEM and TEM images of the CdS nanobelts. The top view in Figure 2a clearly reveals that the products are composed of large amounts of belt-like nanoscaled products. Most of the nanobelts are about tens of micrometer long, and no particles are found at either end of the nanobelts. The inset demonstrates a typical magnified image of the nanobelts with a thickness of about 60 nm and a width of about 400 nm, which is consistent with the TEM image in Figure 2b. The ratio of the thickness-to-width-to-length of the nanobelts is about 1:7:100. Figure 2b exhibits a typical TEM image of a CdS nanobelt, and the inset exhibits the corresponding HRTEM image and the selected area electron diffraction (SAED) pattern. Evidently, the nanobelt is a single crystal and structurally uniform without any dislocation. Moreover, the surface of the nanobelt is very clean and without any sheathed amorphous layer. The lattice spacing of the fringes is 0.67 nm in agreement with the (001) spacing calculated from the diffraction spot in the SAED pattern, which indicates that the CdS nanobelts grow

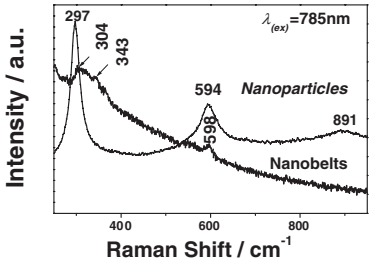

Figure 3. Raman spectra of CdS nanoparticles and nanoblets.

along the [001] direction.

Figure 3 displays the Raman spectra of the CdS nanopaticles and the nanobelts excited at 785 nm. Because of the fluorescence background, the Raman intensities of the CdS nanobelts are very weak, but we still can identify bands at 304 and 598 cm^{-1} corresponding to the first- and the second-order longitudinal optical phonon (LO) modes of CdS, respectively. Compared with those of the pure crystalline CdS,[16] the Raman bands of the nanoparticles have a few red-shifts. Nanda et al.[17] have pointed out that the intensity of the LO mode for CdS decreases with increasing the excitation wavelength of the laser, while the surface phonon (SP) mode blue-shifts at the same time (from 291 to $\approx$330 cm^{-1} by changing the exciting wavelength from 457.9 to 514.5 nm). Therefore, the origin of the band at 343 cm^{-1} should be corresponding to the surface phonon mode, which is confirmed by the XPS results showing a lot of defects on the surface (Cd:S = 57.13:42.87 at%).

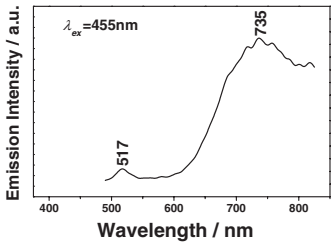

Figure 4. PL spectrum of CdS nanoblets at room temperature.

The photoluminescence (PL) spectrum at room temperature is shown in Figure 4. The excitation wavelength is 455 nm. Two emission bands have been observed around 517 and 735 nm, respectively. The PL behaviors of the CdS nanostructured materials have been studied intensively.[18–22] Burry et al.[19] have reported that two PL bands are observed at 475 and 690 nm, respectively. The band at 475 nm has an intrinsic character, and the other at 690 nm is due to the trap or the surface states. Chrysochoos et al.[22] have revealed that the V_s^+ vacancies are located at about 0.7 eV below the conduction band of the CdS clusters. As the CdS nanobelts are significantly larger than the exciton Bohr diameter ($\approx$6 nm), the band gap of the nanobelts should be similar to that of the bulk CdS materials. So, the band around 517 nm is due to the intrinsic emission. And, according to the calculation, the PL band at 735 nm should be originated from the V_s^+ vacancies, which is confirmed by the XPS results (not showed here).

In conclusion, the CdS nanobelts with high quality and in large area have been fabricated via a rapid evaporation route. The nanobelts have a thickness-to-width-to-length ratio about 1:7:100, and grow along the [001] direction. The PL spectrum of the nanobelts shows two emission bands around 517 and 735 nm, which should arise from the intrinsic transition and the V_s^+ vacancies, respectively. The synthesis method of high-quality CdS nanobelts is very simple with low cost and large production, which will provide the CdS nanobelts potential applications in the optoelectronic devices.

This work is supported by the National Natural Science Foundation of China (NSFC) under grant No.50128202. The authors are grateful to Dr. Changhui Ye for the PL measurements and helpful discussion.

References

1 L. E. Brus, A. L. Efros, and T. Itoh, *J. Lumin*, **76**, 1 (1996).
2 A. M. Morales and C. M. Lieber, *Science*, **279**, 5348 (1998).
3 Z. L. Wang, *Adv. Mater.*, **12**, 1295 (2000).
4 X. F. Duan, Y. Huang, R. Agarwal, and C. M. Lieber, *Nature*, **421**, 6920 (2003).
5 D. Routkevitch, T. L. Hastett, L. Ryan, T. Bigioni, C. Douketis, and M. Moskovits, *Chem. Phys.*, **210**, 343 (1996).
6 S. H. Yu, Y. S. Wu, J. Yang, Z. H. Han, X. Xie, Y. T. Qian, and X. M. Lin, *Chem. Mater.*, **10**, 2309 (1998).
7 Y. W. Jun, S. M. Lee, N. J. Kang, and J. Cheon, *J. Am. Chem. Soc.*, **123**, 5150 (2001).
8 Y. W. Wang, G. W. Meng, L. D. Zhang, C. H. Liang, and J. Zhang, *Chem. Mater.*, **14**, 1773 (2002).
9 C. N. R. Rao, A. Govindaraj, F. Leonard Deepak, and N. A. Gunari, *Appl. Phys. Lett.*, **78**, 1853 (2001).
10 P. Zhang and L. Gao, *Langmuir*, **19**, 208 (2003).
11 Y. J. Xiong, Y. Xie, J. Yang, R. Zhang, C. Z. Wu, and G. Du, *Mater. Chem.*, **12**, 3712 (2002).
12 Z. W. Pan, Z. R. Dai, and Z. L. Wang, *Science*, **291**, 1947 (2001).
13 Y. B. Li, Y. Bando, T. Soto, and K. Kurashima, *Appl. Phys. Lett.*, **81**, 144 (2002).
14 Y. C. Zhu, Y. Bando, and D. F. Yue, *Appl Phys. Lett.*, **82**, 1769 (2003).
15 S. H. Liu, H. W. Lu, X. F. Qian, J. Yin, and Z. K. Zhu, *J. Solid State Chem.*, **172**, 480 (2003).
16 J. S. Sun and J. S. Lee, *Chem. Phys. Lett.*, **281**, 384 (1997).
17 K. K. Nanda, S. N. Sarangi, S. N. Sahu, S. K. Deb, and S. N. Behera, *Physica B*, **262**, 31 (1999).
18 L. Spanhel, M. Haase, H. Weller, and A. Henglein, *J. Am. Chem. Soc.*, **109**, 5649 (1987).
19 J. Butty and N. Peyghambarian, *Appl. Phys. Lett.*, **69**, 3224 (1996).
20 J. H. Zhang, X. G. Yang, D. W. Wang, S. D. Li, Y. Xie, Y. N. Xia, and Y. T. Qian, *Adv. Mater.*, **12**, 13481 (2000).
21 W. Chen, Z. J. Lin, and L. Y. Lin, *Solid State Commun.*, **101**, 371 (1997).
22 J. Chrysochoos, *J. Phys. Chem.*, **96**, 2868 (1992).

Published on the web (Advance View) February 2, 2004; DOI 10.1246/cl.2004.228